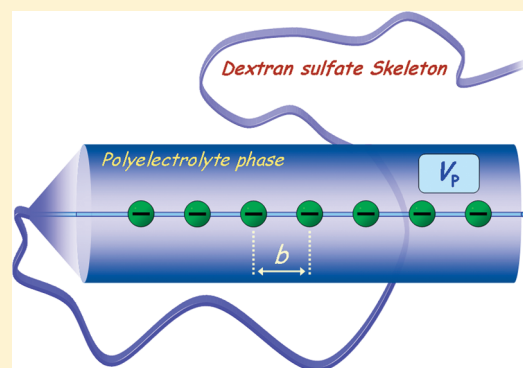


## Linear Charge Density Dependence of the Polyelectrolyte Phase Volume of Ionic Dextran Sulfate as a Strong Acidic Polyion

Hideshi Maki<sup>\*,†</sup> and Tohru Miyajima<sup>‡</sup><sup>†</sup>Department of Chemical Science and Engineering, Graduate School of Engineering, Kobe University, 1-1 Rokkodai-cho, Nada-ku, Kobe, Hyogo 657-8501, Japan<sup>‡</sup>Department of Chemistry, Faculty of Science and Engineering, Saga University, 1-Honjo, Saga 840-8502, Japan

## Supporting Information

**ABSTRACT:** Research on the counterion binding equilibria of the linear polyelectrolytes with anionic groups, i.e., carboxyl, sulfate, or phosphate group, is important for understanding the effect of the electrostatic interaction on the functionalities of polyions. For the analysis of the counterion binding equilibria of polyelectrolytes, the electrostatic interaction between the counterions and the ionic groups fixed on the polymer skeletons should be quantitatively evaluated. In this research, a “two-phase model” which the formation of a polyelectrolyte phase was assumed around the polymer skeleton was applied. In our previous study, it has been confirmed that the Donnan potential and the polyelectrolyte phase volume of weak acidic polyions can be expressed as a function of the average linear charge distance on the polyions. In this work, the divalent metal ion binding equilibria of dextran sulfate anions of different degree of substitution as typical strong acidic polyions was investigated in order to clarify the relationship between the polyelectrolyte phase volume,  $V_p$ , and the average linear charge distance of the negative charge fixed on the strong acidic polyion skeletons. The polyelectrolyte phase volume per fixed ionic group on a polyelectrolyte skeleton,  $V_p/n_p$ , which was estimated by the application of the two-phase model showed a nonmonotonic change against the average linear charge distance,  $1/b$ . The  $V_p/n_p$  increased drastically in  $0 < 1/b < 0.2 \text{ \AA}^{-1}$  and showed the local maximum at  $1/b = \text{ca. } 0.25 \text{ \AA}^{-1}$ . The obtained findings are expected to provide important information for the molecular design of functional polyions of various shapes.



## 1. INTRODUCTION

Counterion binding to polyion systems is of fundamental importance in various fields of science and has long been studied from both theoretical and practical points of view. Among counterion–polyion systems investigated, metal ion binding to polyions with strong acidic groups, such as sulfate and sulfonate groups, is believed to be primarily due to an electrostatic effect;<sup>1–6</sup> counterions are concentrated around the polymer skeleton so as to reduce the electrorepulsive force among the fixed negative charges on the polymer backbone. Applicability of the concept to the analyses of complexation equilibria of weak acidic polyions has fully been documented by Miyajima and co-workers.<sup>7–10</sup> Since the “polyelectrolyte effect” results from the accumulation of the electrostatic effect attributable to individual monomeric ionic groups, which constitute the polymer molecules, it is of interest to study how the ion properties are dependent on the charge density of the polyion.

The following two factors are indispensable to the quantitative evaluation of the electrostatic effect in the counterion binding equilibria of linear polyelectrolytes:<sup>11–15</sup> (1) an ionic strength dependence of the counterion binding equilibria.; (2) a linear polyelectrolyte charge density dependence of the counterion binding equilibria. There is a possibility that the surface charge

density of the polyion domain in a counterion–polyion system varies depending on the ionic strength, and the linear charge density of a polyion has a profound influence on the “polyelectrolyte effect”.<sup>16</sup> However, so far systematic and experimental studies on the dependence of the polyelectrolyte effect of strong acidic polyions on these two factors have been scarce,<sup>17,18</sup> since the ionic groups of strong acidic polyions dissociate almost completely and the linear charge density of strong acidic polyions cannot be changed by the control of any solution conditions (e.g., the pH and temperature of solutions).

Dextran sulfate sodium salt (NaDxS) is a polyanionic derivative of dextran, and the pH of an aqueous solution almost lies between 4 and 7. It is prepared by sulfating a selected fraction of dextran with a normal mean molecular weight greater than 20 000 by purification. Each glucose unit in the dextran chain is able to have maximum three sulfate groups, located at C2, C4, and C3 of the glucose units (Figure S1, Supporting Information); thus, a degree of substitution, DS, that is the average number of sulfate substitution on the glucose unit in the dextran chain can

Received: February 6, 2011

Revised: May 17, 2011

Published: May 27, 2011

vary from 0 to 3. NaDxS is a potent polyanion and as such will interact with cations or polycations, and it is applied to the field of the anticoagulant,<sup>19</sup> acceleration of hybridization rates of DNA fragments,<sup>20–22</sup> lipoprotein remover,<sup>23,24</sup> protein stabilizer, and so on.<sup>25–30</sup> However, most of the studies on the counterion binding equilibria of DxS<sup>−</sup> polyion<sup>2–6</sup> have been carried out by use of a commercially available sample from Pharmacia (Sweden) whose DS is roughly estimated to be 2, and quite a few studies on the effect of the DS on the binding equilibria have been reported.<sup>18</sup>

In this work, the polyelectrolyte effect due to purely electrostatic interaction between the fixed charges on the polymer surface and monovalent (Na<sup>+</sup>) and divalent (Ca<sup>2+</sup>) ions has been evaluated by use of several NaDxS samples of various DS that have been newly synthesized, and the ionic strength dependence of the divalent ion binding behavior of these NaDxS samples with different linear charge densities was examined in order to investigate the transition from neutral polymer to acidic polyions. Two different aspects have been examined: the first is Na<sup>+</sup> ion binding to DxS<sup>−</sup> polyions in the absence of a supporting electrolyte, i.e., the simple Na<sup>+</sup>/DxS<sup>−</sup> system, and the second is divalent metal ion equilibria in the presence of an excess of a supporting electrolyte, i.e., the Ca<sup>2+</sup>/DxS<sup>−</sup>/Na<sup>+</sup>(excess) system. These aspects have been explained by not only thermodynamic measurements of the activities or the concentrations of the counterions but also <sup>23</sup>Na NMR measurements in order to get direct and microscopic information on the bound states of Na<sup>+</sup> ions around the DxS skeletons. The thermodynamic and NMR data thus obtained have been compared with those predicted by Manning,<sup>16</sup> i.e., the correlation between the polyelectrolyte effect and the average linear charge distance between the negative charges fixed on the strong-acid polyions, *b* (Å), has been investigated.

## 2. EXPERIMENTAL METHODS

**2.1. Na<sup>+</sup> Ion Activity (*a*<sub>Na</sub>) Measurement of NaDxS.** *Chemicals.* Sodium dextran sulfate (NaDxS) of different DS values (DS = 0.29, 0.67, 1.14, 1.74, 2.16, and 2.54) were kindly offered by Ph.D. A. Koide of Meito Sangyo (Nagoya, Japan). The DS values of each NaDxS sample were determined from the element molar ratios of carbon to sulfur obtained from elementary analysis. The average molecular weights of the samples are estimated to be about 20 000 by capillary viscometry in a thermostated water bath at 25.0 ± 0.1 °C.<sup>31</sup> Stock solutions of the aqueous solutions of NaDxS have been standardized by an acid–base titration with a standard CO<sub>2</sub>-free NaOH solution, which purchased from Merck, after converting NaDxS into an acidic form by use of a H<sup>+</sup>-form cation exchanger (Dowex 50W × 4) column. Stock solution of NaCl used to calibrate a Na<sup>+</sup> ion selective electrode has been prepared by dissolving analytical grade NaCl purchased from Merck by distilled water, and its molality was determined accurately by gravimetry.

*a*<sub>Na</sub> Measurement by Use of Na<sup>+</sup> Ion Selective Glass Electrode. A Na<sup>+</sup> ion selective glass electrode (Horiba 1512A) and a single-junction reference electrode (Horiba 2010A) were connected to a Horiba N-5 ionalyzer to determine the Na<sup>+</sup> ion activity, *a*<sub>Na</sub>, of NaDxS aqueous solutions. The glass electrode gives the electromotive force, *E*, of the electrochemical cell which can be expressed by a Nernstian equation as follows:

$$E = E_0 + g \log a_{\text{Na}} + E_j \quad (1)$$

where *E*<sub>0</sub> and *E*<sub>j</sub> indicate a standard electrochemical potential and a liquid-junction potential, respectively, and *g* stands for the Nernstian slope. The *E*<sub>j</sub> is estimated to be unvaried during the measurement,<sup>32</sup> and

*E*<sub>0</sub> and *g* have been determined by calibration procedures by use of NaCl solutions of known concentrations, which were carried out just before and after the measurement of the Na<sup>+</sup>–DxS<sup>−</sup> mixture solutions. The *g* values thus determined were 58.5 ± 0.5 mV, being quite close to the theoretical value for univalent ion, 59.15 mV at 25 °C. The pH of the sample solutions and the standard solutions were between 6 and 7, which ensures the negligible interference of hydronium ion on the potential of the Na<sup>+</sup> ion selective glass electrode. All the measurement procedures were carried out at 25.0 ± 0.5 °C.

**2.2. <sup>23</sup>Na NMR Measurements.** <sup>23</sup>Na NMR spectra of Na<sup>+</sup>–DxS<sup>−</sup> mixture solutions were recorded on a JEOL JNM-GX-400 (9.39 T) superconducting FT-NMR spectrometer with a 10 mm tunable broad-band probe and performed at 105.864 MHz. A data acquisition time of resonances was 2 s, the free induction decay of resonances was collected in 105 000 points, and sweep widths were 20 000 Hz, so the digital resolution in the frequency dimension was 0.38 Hz (0.0036 ppm). The Lorentzian line-broadening factor of 1.5 Hz was applied to the total free induction decay prior to Fourier transformation. The NMR chemical shifts were recorded against an external standard of 1.0 mol dm<sup>−3</sup> NaCl in 10% D<sub>2</sub>O. <sup>23</sup>Na NMR spectra of 3 cm<sup>3</sup> portions of 0.005, 0.01, or 0.05 equiv dm<sup>−3</sup> NaDxS in 10% D<sub>2</sub>O were recorded with nondecoupling of <sup>1</sup>H at 25.0 ± 1.0 °C. The <sup>23</sup>Na spin–spin relaxation times, *T*<sub>2</sub>, were measured with the CPMG pulse sequence, 90°<sub>x</sub>–τ–[180°<sub>y</sub>–τ–echo–τ]<sub>n</sub>, as a function of pulse spacing τ.<sup>33–35</sup> In *T*<sub>2</sub> dispersion experiments, the pulse spacing τ of the CPMG sequence was varied between 12 and 5000 μs over 20 values, equally spaced on a logarithmic scale. The number of echoes, *n*, was chosen for each τ to ensure that a stable baseline was reached after the signal had decayed. Scans of 16 times were recorded for each τ by applying a 5 s recycle delay between sequences to avoid saturation and using phase cycling to improve the signal-to-noise ratio. The spinner was turned off to avoid any macroscopic motion. The obtained CPMG echo envelopes were fitted to an exponential function with a nonlinear least-squares curve-fitting method.

**2.3. Measurements of the Free Concentrations of Ca<sup>2+</sup> Ion of the CaCl<sub>2</sub>/NaDxS/NaCl Mixture Solutions.** *Chemicals.* A stock solution of calcium chloride was prepared by dissolving analytical grade calcium chloride hexahydrate, CaCl<sub>2</sub>·6H<sub>2</sub>O, purchased from Merck, and was standardized by the Mohr method (Cl<sup>−</sup> content) and by a volumetric titration with EDTA (Ca<sup>2+</sup> content) using Eriochrome Black T as an indicator. The details of the other chemicals used in this experiment have already been mentioned above.

*Determination of Free Calcium Ion Concentration in the Ca<sup>2+</sup>–DxS<sup>−</sup> Mixture Solutions.* Free Ca<sup>2+</sup> concentrations of the CaCl<sub>2</sub>/NaDxS/NaCl systems have been determined potentiometrically by use of a membrane-type Ca<sup>2+</sup> ion selective electrode (Orion 93-20) and a single junction type reference electrode (Orion 90-01), both connected to an ionalyzer (Orion 720A). All measurements were carried out at 25.0 ± 0.5 °C, keeping the ionic strength, *I*, constant at 0.01, 0.02, 0.05, 0.10, or 0.20 by NaCl. 20 cm<sup>3</sup> portions of 0.01 equiv dm<sup>−3</sup> NaDxS + *I* mol dm<sup>−3</sup> NaCl were titrated stepwise by a solution of 0.01 mol dm<sup>−3</sup> CaCl<sub>2</sub> + *I* mol dm<sup>−3</sup> NaCl, and the stable EMF were measured. All the titration procedures were carried out with an automatic piston buret APB-510 purchased from Kyoto Electronics Manufacturing (Kyoto, Japan) which controlled by a personal computer. The EMF of the electrochemical cell can be expressed by the following equation:

$$E = E_0' + g \log [\text{Ca}^{2+}] \quad (2)$$

where *E*<sub>0</sub>' indicates a standard electrochemical potential of an electrochemical cell and *g* stands for the Nernstian slope. Before and after the titration procedures of the sample solutions, *E*<sub>0</sub>' and *g* were determined by the calibrating titration. 20 cm<sup>3</sup> portions of *I* mol dm<sup>−3</sup> NaCl were titrated stepwise by the solution of 0.01 mol dm<sup>−3</sup> CaCl<sub>2</sub> + *I* mol dm<sup>−3</sup> NaCl, and the stable EMF was measured. The *g* values were 27.0 ± 1.0 mV,

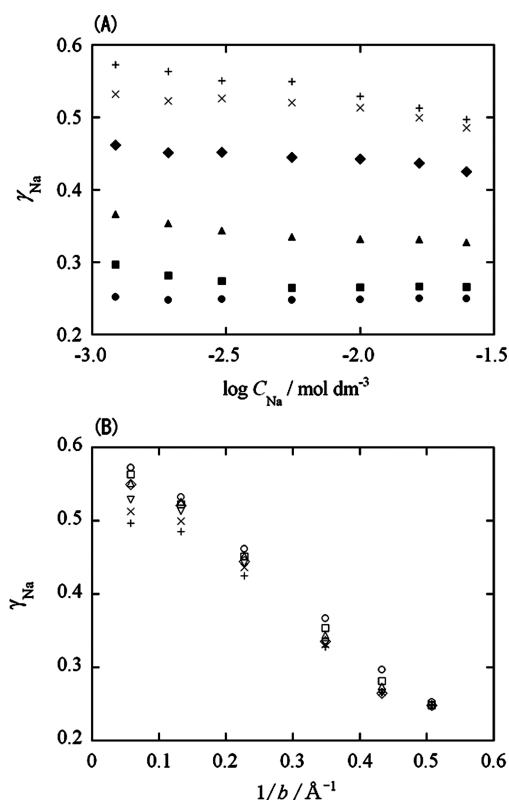


**Figure 1.** (A) Effect of the total concentration on the activity coefficients of  $\text{Na}^+$  ions in the NaDxS aqueous solutions. DS: (●) 2.54; (■) 2.16; (▲) 1.74; (◆) 1.14; (×) 0.67; (+) 0.29. (B) Relationships of the activity coefficients of  $\text{Na}^+$  ions in the NaDxS aqueous solutions and the linear charge densities of  $\text{DxS}^-$  polyions.  $C_{Na}$ : (○)  $1.22 \times 10^{-3} \text{ mol dm}^{-3}$ ; (□)  $1.92 \times 10^{-3} \text{ mol dm}^{-3}$ ; (△)  $3.05 \times 10^{-3} \text{ mol dm}^{-3}$ ; (◇)  $5.56 \times 10^{-3} \text{ mol dm}^{-3}$ ; (▽)  $1.00 \times 10^{-2} \text{ mol dm}^{-3}$ ; (×)  $1.67 \times 10^{-2} \text{ mol dm}^{-3}$ ; (+)  $2.50 \times 10^{-2} \text{ mol dm}^{-3}$ .

being quite close to the theoretical value. Before and after the titration procedures, the pH of the sample solutions was measured to be between 4 and 6, which ensures that all the sulfate groups of  $\text{DxS}^-$  were dissociated completely.

### 3. RESULTS AND DISCUSSION

**3.1.  $\text{Na}^+$  Ion Binding to  $\text{DxS}^-$  Polyions in the Absence of Supporting Electrolyte.** Single ion activity coefficients of  $\text{Na}^+$  ions of  $\text{Na}^+ - \text{DxS}^-$  aqueous solutions,  $\gamma_{Na}$ , can usually be expressed by the following equation:<sup>32,36,37</sup>

$$\gamma_{Na} = \frac{a_{Na}}{[\text{Na}^+]} \quad (3)$$

where  $a_{Na}$  and  $[\text{Na}^+]$  indicate the activity measured potentiometrically and the free  $\text{Na}^+$  ion concentration in the sample solutions, respectively. Since the nature of the binding of  $\text{Na}^+$  ions to  $\text{DxS}^-$  polyions is not covalent site binding but purely electrostatic territorial binding, the  $[\text{Na}^+]$  term in eq 3 can be replaced by the total  $\text{Na}^+$  ion concentration of the NaDxS aqueous solutions,  $C_{Na}$ . The  $\gamma_{Na}$  values thus calculated by the following equation are plotted against  $\log C_{Na}$  as shown in Figure 1A.

$$\gamma_{Na} = \frac{a_{Na}}{C_{Na}} \quad (4)$$

It is noteworthy for all the NaDxS samples of different DS that the  $\gamma_{Na}$  remain constant irrespective of the change in  $\log C_{Na}$ , implying that the  $\gamma_{Na}$  do not approach unity with dilution of the NaDxS aqueous solutions. The similar experimental results have previously been obtained,<sup>18</sup> and this behavior characteristic to the polyelectrolytic nature of the  $\text{DxS}^-$  polyion can be explained as follows. As the  $\text{Na}^+ - \text{polyion}$  solution is diluted, dissociation of  $\text{Na}^+$  ions as counterions is anticipated, whereas this dissociation of  $\text{Na}^+$  ions from the surface of the polyion molecule, on the other hand, increases the overall negative charge density at the polyion surface. These compensating two factors give the almost constant effective surface charge density of the  $\text{Na}^+ - \text{DxS}^-$  system. The  $(1 - \gamma_{Na})$  indicates the fractions of the “bound”  $\text{Na}^+$  ions trapped electrostatically around the polyion skeleton; the values are just dependent on the linear charge density of polyions; i.e., the  $\gamma_{Na}$  can be correlated to the average linear charge distance of polyions,  $b$  (Å). The linear charge density of a polyion,  $1/b$  ( $\text{\AA}^{-1}$ ), can be estimated as follows:

$$\frac{1}{b} = \frac{DS}{d} \quad (5)$$

where  $d$  (Å) indicates the average repeating unit distance of a polyion; in this work, the repeating unit is each glucose ring in a dextran chain, and thus the  $d$  is estimated to be 5 Å. The  $\gamma_{Na}$  values determined by the present study have been plotted in Figure 1B against the  $1/b$  values. It is obvious that the  $\gamma_{Na}$  is only dependent on the  $1/b$  of the polyions. The  $\gamma_{Na}$  decreases with an increase in  $1/b$ , showing that the magnitude of the electrostatic interaction between  $\text{Na}^+$  ions and  $\text{DxS}^-$  polyions increases with an increase in the linear charge density of the polyions.

More microscopic information on the  $\text{Na}^+$  ion binding to  $\text{DxS}^-$  can be obtained by a  $^{23}\text{Na}$  NMR measurement.<sup>38–41</sup> Representative  $^{23}\text{Na}$  NMR spectra obtained in the present study are shown in Figure S2 (Supporting Information). The line widths of the spectra obtained by measuring NaDxS solution are obviously much larger than that obtained with a NaCl aqueous solution of the same concentration. In recent years, Satoh et al. have investigated the counterion binding in Na poly(acrylate) gel by  $^{23}\text{Na}$  NMR and have found out that the ion-pair formations (counterion binding) between strong acidic polyion gel and  $\text{Na}^+$  ions as counterions brought about a downfield shift and an increase of the line width of the  $\text{Na}^+$  nucleus.<sup>42</sup> They have referred to two main contributions for the increase of the line width: the mobility of the ion and the symmetry of the surrounding electric field, both of which enlarge the line width when they decrease.

Since the spin quantum number,  $I_s$ , of  $^{23}\text{Na}$  nuclei is 3/2, the quadrupolar effect is dominant in the transverse relaxation mechanism of  $^{23}\text{Na}$  nuclei. The quadrupole transverse relaxation rate,  $R_{2Q}$ , of a quadrupolar nucleus with spin  $I_s$  situated in a molecule with an isotropic correlation time,  $\tau_c$ , and in the extreme narrowing region is

$$R_2 \approx R_{2Q} = \frac{3(2I_s + 3)}{40I_s^2(2I_s - 1)} \left(1 + \frac{\eta^2}{3}\right) \left(\frac{e^2 q Q}{h}\right)^2 \tau_c \quad (6)$$

where  $Q$  is the quadrupole moment of the nucleus,  $q$  is the electric field gradient around the nucleus,  $\eta$  is the asymmetric parameter of the electric field gradient, and  $e$  and  $h$  are electronic charge and Planck's constant, respectively.<sup>43</sup> In an aqueous solution, the movement of the molecules reduces the distant



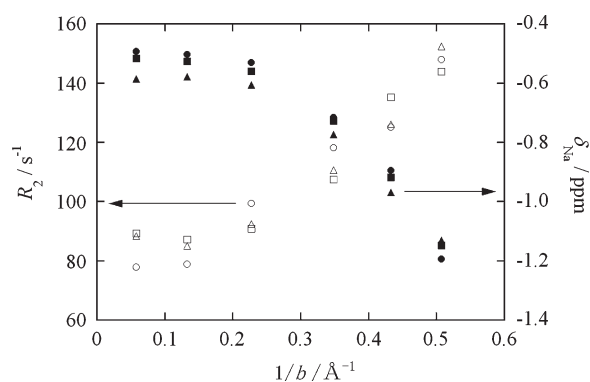


**Figure 2.** Dependence of the  $^{23}\text{Na}$  NMR chemical shifts and the transverse relaxation rates of  $\text{Na}^+$  ions in the  $\text{NaDxS}$  aqueous solutions on the linear charge densities of  $\text{DxS}^-$  polyions. Open symbols,  $^{23}\text{Na}$  NMR chemical shifts; filled symbols, transverse relaxation rates. Concentrations of  $\text{NaDxS}$ : ( $\circ$ ,  $\bullet$ )  $0.005 \text{ equiv dm}^{-3}$ ; ( $\square$ ,  $\blacksquare$ )  $0.01 \text{ equiv dm}^{-3}$ ; ( $\Delta$ ,  $\blacktriangle$ )  $0.05 \text{ equiv dm}^{-3}$ .

effects to 0, and the electric field gradient arises quite locally around the nucleus. Since the  $R_{2Q}$  is determined mainly by the electric field gradient around the nucleus, the  $R_2$  of  $^{23}\text{Na}$  NMR resonance increases depending on the increase of the electric field gradient where  $^{23}\text{Na}$  nuclei are placed. The  $R_2$  and the chemical shifts,  $\delta_{\text{Na}}$ , of the obtained  $^{23}\text{Na}$  NMR resonances are plotted against  $1/b$  in Figure 2 in order to compare with the relationship between the single ion activity coefficient and the  $1/b$  as shown in Figure 1B. As expected, the  $R_2$  increases and the  $\delta_{\text{Na}}$  shows an upfield shift with an increase in the  $1/b$  in accord with the thermodynamic results, reflecting the  $\text{Na}^+$  ion binding to the  $\text{DxS}^-$  surface, whereas one striking different feature between these  $^{23}\text{Na}$  NMR measurements and the thermodynamic results is observed in the region  $0 < 1/b < 0.2$ ; i.e., the  $R_2$  and the  $\delta_{\text{Na}}$  remain unvaried between this region even though the  $\gamma_{\text{Na}}$  tends to decrease with an increase in the linear charge density of the  $\text{DxS}^-$  polyions. This experimental evidence clearly indicates the difference in the nature of the  $\text{Na}^+$  ion bindings to polyions between the two regions, i.e.,  $0 < 1/b < 0.2$  and  $0.2 < 1/b$ .

Recently, Scheler, Stilbs, and Jeschke referred that the new experimental techniques of NMR and EPR,<sup>44</sup> i.e., PFG-NMR,<sup>45</sup> eNMR, and ENDOR, were useful for the direct observation of the counterion condensation on polyions and the nanoscale binding properties of the charge carriers on conducting polymers in their reviews.<sup>46–48</sup> The electrophoretic mobility and quantities derived from it are of considerable interest in polyelectrolyte chemistry because the electrostatic interaction is often the dominant interaction in counterion–polyion systems; thus, the eNMR (electrophoretic NMR) is very suitable for the direct observations of counterion binding properties to polyions, ionic characters of polyions and counterions, and chemical exchanges between free and condensed counterions. Scheler et al. and Paul et al. have determined the kinetic mobilities of poly(styrenesulfonate) and tetramethylammonium counterions in micellar solutions<sup>49,50</sup> with an eNMR. Furthermore, Grass et al. have estimated the effective charge in dependence of the degree of polymerization,  $D$ , of polyelectrolytes with an eNMR and have found out that the effective charge for long-chain polyelectrolytes ( $D > 10$ ) is in good agreement with Manning's prediction as follows.<sup>51</sup>

According to Manning's ion-condensation theory,<sup>52</sup> a dimensionless structural parameter,  $\xi$ , is defined for a polyion as

follows:

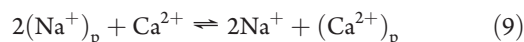
$$\xi = \frac{e^2}{\epsilon b k T} \quad (7)$$

where  $\epsilon$ ,  $k$ , and  $T$  indicate the dielectric constant of the solvent, Boltzmann's constant, and the thermodynamic temperature of the solution, respectively. At  $25^\circ\text{C}$  in an aqueous solution,  $\xi$  is expressed as  $7.14/b$  and the condensation of  $\text{A}^{N+}$  ion to the polyion surface is observed when  $\xi > 1/N$ . In the case of monovalent cations, i.e.,  $N = 1$ , condensation is expected when  $\xi > 1$ , namely,  $1/b > 0.14$ . This transition point that is predicted by Manning found in the present  $^{23}\text{Na}$  NMR measurements indicates that the ion-condensation theory can be applied to the  $\text{Na}^+ - \text{DxS}^-$  binding.

**3.2. Divalent Metal Ion Binding to Polyions in the Presence of Excess Uniunivalent Supporting Electrolyte.** In order to express the degree of binding to polyions, binding isotherms have been obtained at different concentrations of  $\text{NaCl}$  as supporting electrolyte. Representative binding isotherms, i.e., the plots of  $\theta_{\text{Ca}}$  vs  $\log[\text{Ca}^{2+}]$ , obtained for  $\text{DxS}^-$  ( $DS = 0.29, 1.14$ , and  $2.16$ ) polyion are shown in Figure 3A. The average number of bound  $\text{Ca}^{2+}$  ions,  $\theta_{\text{Ca}}$ , per fixed ionic group of polyions, can be calculated as follows:

$$\theta_{\text{Ca}} = \frac{C_{\text{Ca}} - [\text{Ca}^{2+}]}{C_{\text{p}}} \quad (8)$$

where  $C_{\text{Ca}}$  and  $C_{\text{p}}$  indicate total concentrations of  $\text{Ca}^{2+}$  ions and fixed ionic groups on the polyions, respectively. Enlightening in Figure 3A is the parallel relationship of the binding isotherms obtained at different supporting electrolyte concentrations. The increase in  $\text{NaCl}$  concentration suppress the binding of  $\text{Ca}^{2+}$  ion to the polyions due to the electrostatic shielding of  $\text{Na}^+$  ion on the polyion surface, which causes a shift of the binding isotherms to the right-hand side. In order to examine this effect quantitatively, the  $\theta_{\text{Ca}}$  are replotted against  $\log[\text{Ca}^{2+}] - 2 \log[\text{Na}^+]$  as shown in Figure 3B. The convergence of the binding isotherms to respective single curves implies that at a certain  $\theta_{\text{Ca}}$ , thus the  $[\text{Ca}^{2+}]/[\text{Na}^+]^2$  quotient terms that can be derived from  $\log[\text{Ca}^{2+}] - 2 \log[\text{Na}^+]$  are closely related to  $\theta_{\text{Ca}}$ . It has previously been pointed out this relationship is commonly observed for any combinations of metal ions, supporting electrolytes, and highly charged linear polyions, and can be explained by assuming ion-exchange equilibria of counterions between a polyelectrolyte phase formed around the polymer skeleton and the bulk solution phase.<sup>1</sup> A selectivity coefficient,  $K_{\text{ex}}$ , to express the ion-exchange equilibrium reaction



can be expressed as

$$K_{\text{ex}} = \frac{[\text{Ca}^{2+}]_{\text{p}}[\text{Na}^+]^2}{[\text{Ca}^{2+}][\text{Na}^+]_{\text{p}}^2} \quad (10)$$

where "p" indicates the polyelectrolyte phase. Since the  $K_{\text{ex}}$  value and the ratio  $[\text{Ca}^{2+}]_{\text{p}}/[\text{Na}^+]_{\text{p}}^2$  can be regarded constant at a specified  $\theta_{\text{Ca}}$ , the constancy of the  $[\text{Ca}^{2+}]/[\text{Na}^+]^2$  term can be rationalized by the ion-exchange model.

For example, in the Donnan approach,<sup>53–60</sup> a polyion is considered to behave as an electrically neutral polyelectrolyte phase having a particular volume throughout which there is a uniform averaged electrostatic potential known as the Donnan

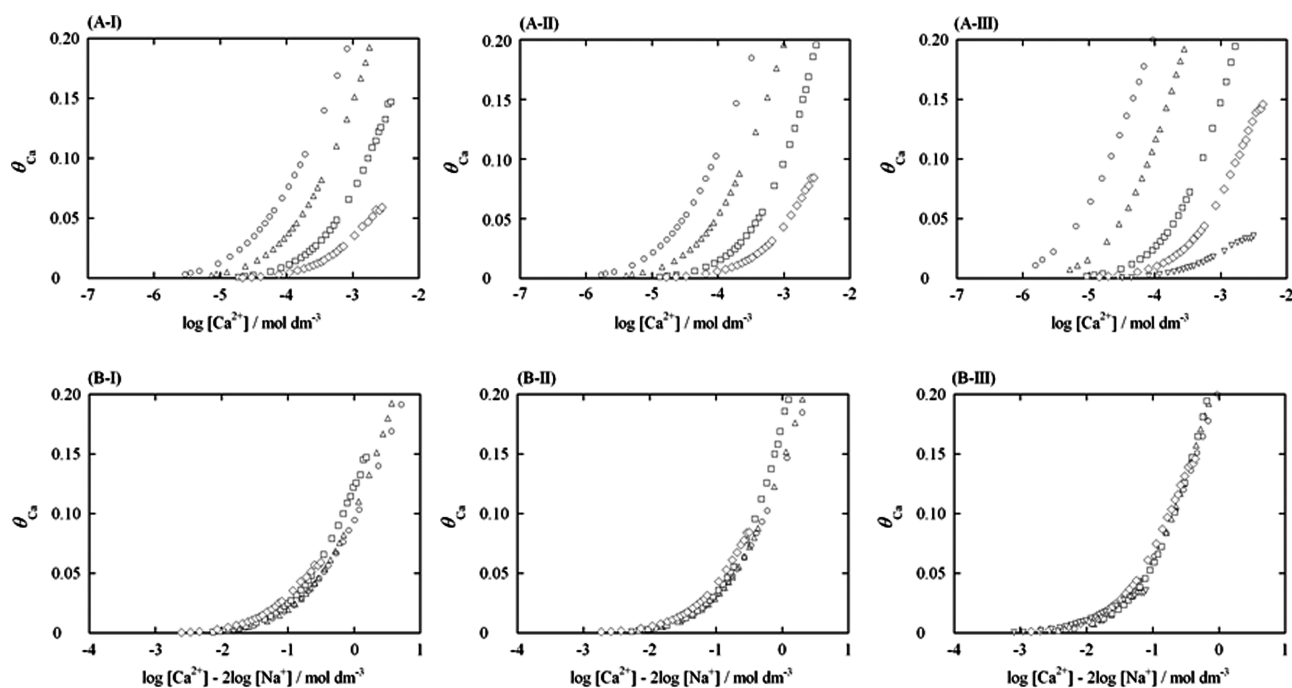


**Figure 3.** (A) Representative binding isotherms of  $\text{CaCl}_2/\text{NaDxS}/\text{NaCl}$  system. (B) Representative plots of  $\theta_{\text{Ca}}$  against  $\log [\text{Ca}^{2+}] - 2 \log [\text{Na}^+]$  for the  $\text{CaCl}_2/\text{NaDxS}/\text{NaCl}$  system. Degree of substitution of  $\text{NaDxS}$  (DS): (I)  $\text{DS} = 0.29$ ; (II)  $\text{DS} = 1.14$ ; (III)  $\text{DS} = 2.16$ . Ionic strengths: (O)  $0.01 \text{ mol dm}^{-3}$ ; ( $\Delta$ )  $0.02 \text{ mol dm}^{-3}$ ; ( $\square$ )  $0.05 \text{ mol dm}^{-3}$ ; ( $\diamond$ )  $0.10 \text{ mol dm}^{-3}$ ; ( $\nabla$ )  $0.20 \text{ mol dm}^{-3}$ .

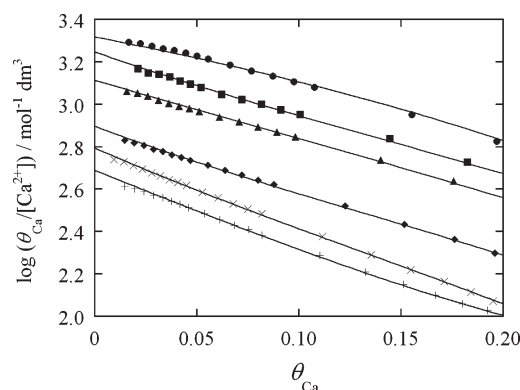


**Figure 4.** Representative relationships of  $\log(\theta_{\text{Ca}}/[\text{Ca}^{2+}])$  as the extrinsic binding constants and  $\theta_{\text{Ca}}$ . The  $\log K_{\text{Ca}}^0$  as the intrinsic binding constants can be determined by extrapolating to  $\theta_{\text{Ca}} = 0$ . DS: (●) 2.54; (■) 2.16; (▲) 1.74; (◆) 1.14; (×) 0.67; (+) 0.29.  $I = 0.02 \text{ mol dm}^{-3}$ .

potential. In this work, it is of special to evaluate the polyelectrolyte phase volume of such a water-soluble polyion system by use of these binding data. In order to make possible the computation of the  $V_p$  value, an intrinsic binding constant,  $K_{\text{Ca}}^0$  is defined by the following equation for respective experimental condition:

$$K_{\text{Ca}}^0 = \lim_{\theta_{\text{Ca}} \rightarrow 0} \frac{\theta_{\text{Ca}}}{[\text{Ca}^{2+}]} \quad (11)$$

The plots of  $\theta_{\text{Ca}}/[\text{Ca}^{2+}]$  vs  $\theta_{\text{Ca}}$  to determine the extrapolated value of  $K_{\text{Ca}}^0$  are the well-known Scatchard plots;<sup>61–66</sup> in this work, the  $\log K_{\text{Ca}}^0$  has been determined by extrapolating to  $\theta_{\text{Ca}} = 0$  of the  $\log(\theta_{\text{Ca}}/[\text{Ca}^{2+}])$  versus  $\theta_{\text{Ca}}$  plots as shown in Figure 4, and all the values are listed in Table 1. The  $\log K_{\text{Ca}}^0$  thus obtained are plotted against the linear charge density of the  $\text{DxS}^-$  polyion,  $1/b$ , as

shown in Figure S3 (Supporting Information), in order to confirm whether the transition can be observed in the divalent cation binding to  $\text{DxS}^-$  polyions in the presence of excess supporting electrolyte, as has been discussed in the  $^{23}\text{Na}$  NMR measurements. It is obvious from these plots that the  $\log K_{\text{Ca}}^0$  decreases with a decrease in the linear charge density; however, after at a certain point, i.e.,  $1/b = \text{ca. } 0.25 \text{ \AA}^{-1}$ , the decrease in the  $\log K_{\text{Ca}}^0$  cannot be observed in spite of the decrease in the  $1/b$ . Note that no transition has been observed in the single activity measurement of  $\text{Na}^+$  ions in the  $\text{Na}^+ - \text{DxS}^-$  system, whereas the transition has clearly been observed in the divalent metal ion binding equilibria in the presence of an excess supporting electrolyte, i.e., the ion-exchange system. In order to express this ion-exchange nature of the divalent metal ion binding to the  $\text{DxS}^-$  polyions, the  $\log K_{\text{Ca}}^0$  are plotted against the  $\log [\text{Na}^+]$  as shown in Figure 5; the plots give straight lines for respective the  $\text{DxS}^-$  polyions, whose slopes are quite close to “−2”. According to the “two-phase model” as representative of the ion-exchange model, the following equation can be applied.<sup>1</sup>

$$\frac{(a_{\text{Ca}})_p}{a_{\text{Ca}}} = \left\{ \frac{(a_{\text{Na}})_p}{a_{\text{Na}}} \right\}^2 \quad (12)$$

Since the driving force for  $\text{Ca}^{2+}$  ion binding to  $\text{DxS}^-$  polyions is purely electrostatic, the activities of  $\text{Ca}^{2+}$  and  $\text{Na}^+$  ions in the polyion domain,  $(a_{\text{Ca}})_p$  and  $(a_{\text{Na}})_p$ , can be expressed as follows:

$$(a_{\text{Ca}})_p = (\gamma_{\text{Ca}})_p [\text{Ca}^{2+}]_p = (\gamma_{\text{Ca}})_p \theta_{\text{Ca}} \frac{n_p}{V_p} \quad (13)$$

$$\begin{aligned} (a_{\text{Na}})_p &= (\gamma_{\text{Na}})_p [\text{Na}^+]_p \\ &= (\gamma_{\text{Na}})_p (1 - \phi_{p,\text{Na}} - 2\theta_{\text{Ca}}) \frac{n_p}{V_p} \end{aligned} \quad (14)$$

**Table 1.** Intrinsic Binding Constants,  $\log K_{Ca}^0$  ( $\text{mol}^{-1} \text{dm}^3$ ), for  $\text{CaCl}_2/\text{NaDxS}/\text{NaCl}$  System Determined by Extrapolating to  $\theta_{Ca} = 0$  of the  $\log(\theta_{Ca}/[\text{Ca}^{2+}])$  vs  $\theta_{Ca}$  Plots<sup>a</sup> ( $T = 25.0 \pm 0.5$  °C)

DS	$1/b$ ( $\text{\AA}^{-1}$ ) <sup>b</sup>	$I = 0.01$	$I = 0.02$	$I = 0.05$	$I = 0.10$	$I = 0.20$
0.29	0.058	$3.38 \pm 0.02$	$2.69 \pm 0.02$	$2.05 \pm 0.01$	$1.67 \pm 0.01$	— <sup>c</sup>
0.67	0.13	$3.49 \pm 0.02$	$2.80 \pm 0.02$	$2.13 \pm 0.01$	$1.73 \pm 0.01$	— <sup>c</sup>
1.14	0.23	$3.54 \pm 0.02$	$2.91 \pm 0.02$	$2.19 \pm 0.01$	$1.79 \pm 0.01$	— <sup>c</sup>
1.74	0.35	$3.78 \pm 0.02$	$3.12 \pm 0.02$	$2.36 \pm 0.01$	$1.93 \pm 0.01$	$1.61 \pm 0.01$
2.16	0.43	$3.89 \pm 0.02$	$3.23 \pm 0.02$	$2.45 \pm 0.01$	$2.00 \pm 0.01$	$1.49 \pm 0.01$
2.54	0.51	$3.95 \pm 0.02$	$3.30 \pm 0.02$	$2.53 \pm 0.02$	$2.07 \pm 0.01$	$1.44 \pm 0.01$

<sup>a</sup>The errors estimated in the listed values are based on the errors in the extrapolating the  $\log(\theta_{Ca}/[\text{Ca}^{2+}])$  vs  $\theta_{Ca}$  plots as shown in Figure 4.

<sup>b</sup>Determined by eq 5. <sup>c</sup>Electrostatic counterion binding to  $\text{DxS}^-$  polyion was scarcely formed.

where  $n_p$  stands for the total amount of ionic sulfate groups of the  $\text{DxS}^-$  polyions expressed in equivalent,  $V_p$  stands for the polyelectrolyte phase volume around the molecular skeleton of a polyion, and  $\phi_{p,Na}$  is the osmotic coefficient of the polyion. The “ $-\phi_{p,Na}$ ” term of eq 14 shows that a significant fraction of  $\text{Na}^+$  ions as counterions moves against an condensed electric field around a polyion,<sup>67–71</sup> and the “ $-2\theta_{Ca}$ ” term is based on the electrical neutralization in the cation-exchange process of the  $\text{Ca}^{2+}/\text{DxS}^-/\text{Na}^+$  system as expressed in eq 9. Substituting eqs 13 and 14 for eq 12 and rearranging the resultant equation, we obtain the following equation:

$$\frac{V_p}{n_p} = \frac{\gamma_{Ca}}{(\gamma_{Ca})_p} \left\{ \frac{(\gamma_{Na})_p}{\gamma_{Na}} \right\}^2 \frac{[\text{Ca}^{2+}]}{[\text{Na}^+]^2} \frac{(1 - \phi_{p,Na} - 2\theta_{Ca})^2}{\theta_{Ca}} \quad (15)$$

By extrapolating  $\theta_{Ca}$  to 0, we can express the  $V_p/n_p$  term as follows:

$$\frac{V_p}{n_p} = \frac{\gamma_{Ca}}{(\gamma_{Ca})_p} \left\{ \frac{(\gamma_{Na})_p}{\gamma_{Na}} \right\}^2 \frac{(1 - \phi_{p,Na})^2}{K_{Ca}^0 [\text{Na}^+]^2} \quad (16)$$

This is the equation to determine the specific polyelectrolyte phase volume,  $V_p/n_p$ , of polyions by use of the intrinsic binding constant,  $K_{Ca}^0$ .<sup>66</sup> It should be noted that the  $V_p$  term can be evaluated only the asymmetrical ion-exchange system (e.g.,  $\text{Ca}^{2+}/\text{Na}^+$ ,  $\text{Ca}^{2+}/\text{K}^+$ ,  $\text{Mg}^{2+}/\text{Na}^+$ ) because the  $V_p/n_p$  term does not remain when eqs 13 and 14 are substituted for eq 12 in a symmetrical ion-exchange system (e.g.,  $\text{Na}^+/\text{K}^+$ ,  $\text{Li}^+/\text{Na}^+$ ,  $\text{Li}^+/\text{K}^+$ ). The  $\phi_{p,Na}$  values for acidic polysaccharides of different charge densities have previously been reported by Katchalsky and co-workers,<sup>67</sup> and the values necessary for the  $V_p$  computation have been obtained by interpolating the curve shown in their reference.<sup>67</sup>

Equation 16 contains the activity coefficients of  $\text{Ca}^{2+}$  ions in the polyion domain, which can be calculated by a proper assessment of the ionic strengths in the polyion domain. The ionic strength of the polyion domain,  $I_p$ , can be calculated by an extrathermodynamic way as follows:

$$I_p = \frac{1}{2}([\text{Na}^+]_p + [\text{SO}_3^-]_p) \\ = \frac{1}{2} \left\{ (1 - \phi_{p,Na}) \frac{n_p}{V_p} + \frac{n_p}{V_p} \right\} = \left( 1 - \frac{\phi_{p,Na}}{2} \right) \frac{n_p}{V_p} \quad (17)$$

In order to determine the  $V_p$ , a successive approximation procedure is adopted. For the first approximation, the activity coefficient quotient,  $\{\gamma_{Ca}/(\gamma_{Ca})_p\} \{(\gamma_{Na})_p/\gamma_{Na}\}^2$ , is estimated to be unity, and the first  $V_p$  value is calculated by eq 16. By use of

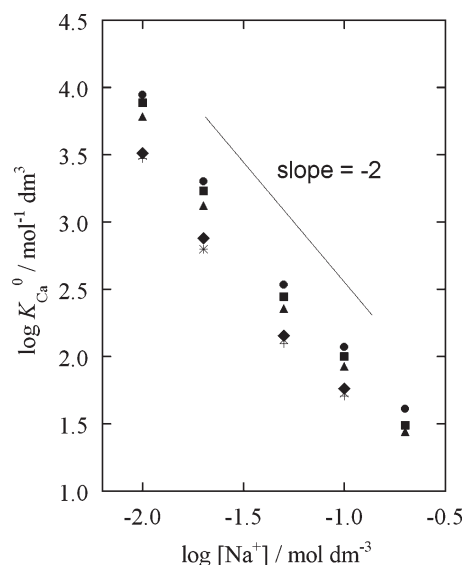


**Figure 5.** Correlation of the  $\log K_{Ca}^0$  and the  $\log [\text{Na}^+]$  in  $\text{CaCl}_2/\text{NaDxS}/\text{NaCl}$  ion-exchange system. The slope of the additional straight line is  $-2$ . DS: (●) 2.54; (■) 2.16; (▲) 1.74; (◆) 1.14; (×) 0.67; (+) 0.29.

this approximated  $V_p$  value, the first approximated  $I_p$  value is calculated by eq 17. The activity coefficients of  $\text{Ca}^{2+}$  and  $\text{Na}^+$  ions in the  $\text{DxS}^-$  polyion domain,  $(\gamma_{Ca})_p$  and  $(\gamma_{Na})_p$ , are then evaluated by use of the first approximated  $I_p$  value. Since the mean activity coefficients of the salts  $\text{CaCl}_2$  and  $\text{NaCl}$  are available in the literature,<sup>72</sup> the respective single ion activity coefficients have been calculated by assuming  $\gamma_{K^+} = \gamma_{Cl^-}$ . The respective single ion activity coefficients under ionic strengths lower than 0.10 are obtained from Kielland's table.<sup>73</sup> After evaluating the single ion activity coefficients respective  $\gamma$  values in the polyion domain,  $(\gamma_{Ca})_p$  and  $(\gamma_{Na})_p$ , the second approximated  $V_p$  value can be computed by eq 16, which enables again to calculate the second approximated  $I_p$  value by eq 17. By continuing this calculation, we can obtain finally a self-convergence  $V_p/n_p$  value.

The  $V_p/n_p$  thus determined for different DS of  $\text{DxS}^-$  polyions at different supporting electrolyte concentrations are all listed in Table 2 together with the original  $\log K_{Ca}^0$  used for the computation. The  $V_p/n_p$  are dependent on the linear charge density of the  $\text{DxS}^-$  polyions. On the other hand, at low supporting electrolyte concentrations as 0.01–0.02  $\text{mol dm}^{-3}$ , the  $V_p/n_p$  seem to remain constant. As the supporting electrolyte concentration

**Table 2.** Polyelectrolyte Phase Volume,  $V_p/n_p$  ( $\text{cm}^3 \text{equiv}^{-1}$ ), for  $\text{DxS}^-$  Polyions in  $\text{CaCl}_2/\text{NaDxS}/\text{NaCl}$  Ion-Exchange System Determined by a Successive Approximation Procedure<sup>a</sup> ( $T = 25.0 \pm 0.5$  °C)

DS	$1/b$ ( $\text{\AA}^{-1}$ ) <sup>b</sup>	$I = 0.01$	$I = 0.02$	$I = 0.05$	$I = 0.10$	$I = 0.20$
0.29	0.058	$0.73 \pm 0.02$	$0.74 \pm 0.02$	$0.56 \pm 0.02$	$0.34 \pm 0.01$	— <sup>c</sup>
0.67	0.13	$1.43 \pm 0.03$	$1.65 \pm 0.03$	$1.18 \pm 0.03$	$0.72 \pm 0.02$	— <sup>c</sup>
1.14	0.23	$2.08 \pm 0.04$	$2.11 \pm 0.04$	$1.67 \pm 0.03$	$1.02 \pm 0.02$	— <sup>c</sup>
1.74	0.35	$1.63 \pm 0.03$	$1.76 \pm 0.04$	$1.52 \pm 0.03$	$0.99 \pm 0.03$	$0.73 \pm 0.02$
2.16	0.43	$1.45 \pm 0.03$	$1.53 \pm 0.03$	$1.39 \pm 0.03$	$0.94 \pm 0.02$	$0.73 \pm 0.02$
2.54	0.51	$1.38 \pm 0.03$	$1.43 \pm 0.03$	$1.25 \pm 0.03$	$0.87 \pm 0.02$	$0.61 \pm 0.02$

<sup>a</sup>The details of a successive approximation procedure are given in the text. The errors estimated in the listed  $V_p/n_p$  values are based on the errors in the evaluation of the  $\log K_{\text{Ca}}^0$  values which are listed in Table 1. <sup>b</sup>Determined by eq 5. <sup>c</sup>Electrostatic counterion binding to  $\text{DxS}^-$  polyion was scarcely formed.

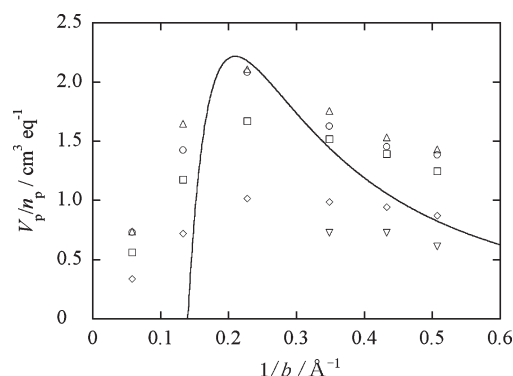


**Figure 6.** Variation in the polyelectrolyte phase volume for  $\text{DxS}^-$  polyions in  $\text{CaCl}_2/\text{NaDxS}/\text{NaCl}$  ion-exchange system with the linear charge densities of the polyions. Solid line refers to the theoretical value which calculated by Manning's "two variable theory".<sup>16</sup> Ionic strengths: (○) 0.01  $\text{mol dm}^{-3}$ ; (△) 0.02  $\text{mol dm}^{-3}$ ; (□) 0.05  $\text{mol dm}^{-3}$ ; (◇) 0.10  $\text{mol dm}^{-3}$ ; (▽) 0.20  $\text{mol dm}^{-3}$ .

increases as high as 0.10–0.20  $\text{mol dm}^{-3}$ , the  $V_p/n_p$  begin to decrease, since the polyelectrolyte phase around the  $\text{DxS}^-$  polyions will shrink at the high supporting electrolyte concentration by the electrostatic neutralization due to the binding of  $\text{Na}^+$  ions as supporting cations to the surface of the  $\text{DxS}^-$  polyion domain.

It is of a great concern to examine the effect of linear charge density on the magnitude of the  $V_p/n_p$ . In Figure 6, the change in the  $V_p/n_p$  with the  $1/b$  is shown. It is obvious that the relationship between the  $V_p/n_p$  and the  $1/b$  is not monotonous, but a transition is clearly observed at a certain  $1/b$  value, i.e.,  $1/b = \text{ca. } 0.25 \text{ \AA}^{-1}$ . As has already been stated, this transition reflects the transition observed in the  $\log K_{\text{Ca}}^0$  vs  $1/b$  plots as Figure S3 (Supporting Information). Manning has predicted the transition of the  $V_p/n_p$  dependence on the linear charge density by his "two variable theory"<sup>16,74–76</sup> as a purely electrostatic binding theory that  $V_p/n_p$  is expressed only as a function of  $b$  ( $\text{\AA}$ ) of a linear polyion as follows:<sup>16</sup>

$$\frac{V_p}{n_p} = 41.1 \left( \frac{7.14}{b} - 1 \right) b^3 \quad (18)$$

Then, from the formula for the derivative

$$\frac{1}{n_p} \frac{dV_p}{db} = 41.1 \left( \frac{14.28}{b} - 3 \right) b^2 \quad (19)$$

This equation indicates that the polyelectrolyte phase volume vanishes at  $1/b = 0.140$  and shows maximum at  $1/b = 0.210$ . The solid line shown in Figure 6 corresponds to the calculated curve due to eq 18 and obviously indicates these features of the theoretical  $V_p/n_p$  value. The consistency of the exact magnitude of the polyelectrolyte phase volume between the theory and the present experimental results clearly indicates the validity of the present computation procedures to evaluate the hypothetical polyelectrolyte phase volume based on the Donnan distribution of counterions. The inconsistency observed in the lowly linear charge density of  $\text{DxS}^-$  sample ( $1/b = 0.058 \text{ \AA}^{-1}$ ) may partly be due to the heterogeneous distribution of the ionic sulfate groups fixed on the dextran backbone. It has been verified by the present work that the polyelectrolyte phase volume evidently increases for the  $\text{DxS}^-$  polyions whose linear charge density is definitely higher than a certain value, i.e.,  $1/b = \text{ca. } 0.10 \text{ \AA}^{-1}$ , shows a maximum at  $1/b = \text{ca. } 0.25 \text{ \AA}^{-1}$  and tends to decrease with an increase in the linear charge density in  $1/b > 0.25 \text{ \AA}^{-1}$ . The exact magnitude of the  $\text{DxS}^-$  polyion domain is approximately 1–2  $\text{cm}^3 \text{equiv}^{-1}$ , implying that the nature of the  $\text{DxS}^-$  polyion domain can be approximately estimated as a concentrated electrolyte solution by eq 17 in the successive approximation of the determine the  $V_p$  value, whose ionic strength is ca. 0.5–1.0  $\text{mol dm}^{-3}$ . Assuming a cylindrical geometry of the  $\text{DxS}^-$  polyelectrolyte phase volume around the linear dextran backbone, the radius of the polyion domain cylinder can be calculated as 10–15  $\text{\AA}$ .

#### 4. CONCLUSIONS

The divalent metal ion binding to  $\text{DxS}^-$  polyions has been suppressed very regularly by the increase in the  $\text{NaCl}$  concentration due to the electrostatic shielding of  $\text{Na}^+$  ion on the polyion surface. It can be explained by assuming ion-exchange equilibria of counterions between a polyelectrolyte phase formed around the  $\text{DxS}$  polymer skeleton and a bulk solution phase.

Both continuity and discontinuity were observed in the  $\text{Na}^+$  ion and  $\text{Ca}^{2+}$  ion binding properties of  $\text{DxS}^-$  of different linear charge densities. Continuity was observed in the measurement of a  $\text{Na}^+$  singleion activity coefficient of the sodium salts of the  $\text{DxS}^-$  in the absence of supporting electrolyte; the activity coefficient decreases continuously with the increase in the linear charge density. Microscopic information, on the other hand, of the  $\text{Na}^+$  ion binding to the  $\text{DxS}^-$  monitored by the change of the transverse relaxation rate,  $R_2$ , of the obtained  $^{23}\text{Na}$  NMR resonances obviously indicates a clear discontinuity in the bound state of  $\text{Na}^+$  ion around the dextran skeleton. Both the intrinsic binding constants,  $\log K_{\text{Ca}}^0$ , and the specific polyelectrolyte phase



volume,  $V_p/n_p$ , in the  $\text{Ca}^{2+}$  ion binding equilibria of the  $\text{Ca}^{2+}/\text{DxS}^-/\text{Na}^+$  system also showed discontinuity at a certain linear charge density of the  $\text{DxS}^-$ , i.e.,  $1/b = \text{ca. } 0.25 \text{ \AA}^{-1}$ . All discontinuity is consistent with the Manning's prediction on "two variable theory",<sup>16,74–76</sup> indicating that ion condensation around the polyion molecules appears only in  $1/b > 0.140 \text{ \AA}^{-1}$  and shows maximum at  $1/b = 0.210 \text{ \AA}^{-1}$ .

In order to investigate further the particular counterion binding behavior, the  $\text{Li}^+$  ion and  $\text{La}^{3+}$  ion binding properties of  $\text{DxS}^-$  polyions are now being studied by  $^7\text{Li}$  NMR and the colorimetric method in our laboratory. According to the two-variable theory, it can be expected that the  $V_p/n_p$  will not depend on the charge of the counterion in the ion-exchange equilibria between the polyelectrolyte phase and the bulk solution phase.

## ■ ASSOCIATED CONTENT

**S Supporting Information.** Generalized structure of ionic  $\text{DxS}^-$  polyion unit,  $^{23}\text{Na}$  NMR spectra of the  $0.01 \text{ equiv dm}^{-3}$   $\text{NaDxS}$  aqueous solutions, and plots of the dependence of the  $\log K_{\text{Ca}}$  for the  $\text{CaCl}_2/\text{NaDxS}/\text{NaCl}$  system on the linear charge densities of  $\text{DxS}^-$  polyions,  $1/b$ . This material is available free of charge via the Internet at <http://pubs.acs.org>.

## ■ AUTHOR INFORMATION

### Corresponding Author

\*E-mail: [maki@kobe-u.ac.jp](mailto:maki@kobe-u.ac.jp).

## ■ REFERENCES

- Marinsky, J. A.; Baldwin, R.; Reddy, M. M. *J. Phys. Chem.* **1985**, *89*, 5303.
- Kwak, J. C. T.; Joshi, Y. M. *Biophys. Chem.* **1981**, *13*, 55.
- Joshi, Y. M.; Kwak, J. C. T. *Biophys. Chem.* **1981**, *13*, 65.
- Mattai, J.; Kwak, J. C. T. *Biophys. Chem.* **1981**, *14*, 55.
- Mattai, J.; Kwak, J. C. T. *J. Phys. Chem.* **1984**, *88*, 2625.
- Mattai, J.; Kwak, J. C. T. *J. Phys. Chem.* **1982**, *86*, 1026.
- Miyajima, T. *Ion Exchange and Solvent Extraction*; Marcel Dekker: New York, 1995; Vol. 12, Chapter 7.
- Miyajima, T.; Mori, M.; Ishiguro, S.; Chung, K. H.; Moon, C. H. *J. Colloid Interface Sci.* **1996**, *184*, 279.
- Miyajima, T.; Mori, M.; Ishiguro, S. *J. Colloid Interface Sci.* **1997**, *187*, 259.
- Miyajima, T. *Metal Complexation in Polymer Systems*; Marcel Dekker: New York, 1999; Chapter 8.
- Liao, Q.; Dobrynin, A. V.; Rubinstein, M. *Macromolecules* **2003**, *36*, 3399.
- Böhme, U.; Scheler, U. *Colloids Surf., A* **2003**, *222*, 35.
- Böhme, U.; Scheler, U. *Adv. Colloid Interface Sci.* **2010**, *158*, 63.
- Deshkovski, A.; Obukhov, S.; Rubinstein, M. *Phys. Rev. Lett.* **2001**, *86*, 2341.
- Dobrynin, A. V.; Deshkovski, A.; Rubinstein, M. *Macromolecules* **2001**, *34*, 3421.
- Manning, G. S. *Q. Rev. Biophys.* **1978**, *2*, 179.
- Satake, I.; Fukuda, M.; Ohta, T.; Nakamura, K.; Fujita, N.; Yamauchi, A.; Kimizuka, H. *J. Polym. Sci.* **1972**, *10*, 2343.
- Noguchi, H.; Gekko, K.; Makino, S. *Macromolecules* **1973**, *6*, 438.
- Grönwall, A.; Ingelman, B.; Mosimann *Uppsala Läkarförening Förh.* **1945**, *54*, 397.
- Wahl, G. M.; Stern, M.; Stark, G. R. *Proc. Natl. Acad. Sci. U.S.A.* **1979**, *76*, 3683.
- Sambrook, F.; et al. *Molecular Cloning: A Laboratory Manual*, 2nd ed.; Cold Spring Harbor: New York, 1989; Chapter 11.
- Wetmur, J. G. *Biopolymers* **1975**, *14*, 2517.
- Oncley, J. L.; Walton, K. W.; Cornwell, D. G. *J. Am. Chem. Soc.* **1957**, *79*, 4666.
- Yokohama, S.; Hayashi, R.; Satani, M.; Yamamoto, A. *Arterioscler. Thromb. Vasc. Biol.* **1985**, *5*, 613.
- Schlorlemmer, H. U.; Burger, R.; Hylton, W.; Allison, A. C. *Clin. Immunol. Immunopathol.* **1977**, *7*, 88.
- Hadding, U.; Dierich, M.; König, W. *Eur. J. Immunol.* **1973**, *3*, 527.
- Kettman, J.; Söderberg, A.; Lefkovits, I. *Cell. Immunol.* **1984**, *88*, 129.
- Hahn, H.; Bierther, M. *2nd Workshop Conference Hoechst*; Elsevier: New York, 1974; p 249.
- Hilgers, L. A.; Snippe, H.; Jansze, M.; Willers, J. M. *Cell. Immunol.* **1985**, *92*, 203.
- Baba, M.; Snoeck, R.; Pauwels, R.; de Clerq, E. *Antimicrob. Agents Chemother.* **1988**, *32*, 1742.
- Wan, P. J.; Adams, E. T., Jr. *Biophys. Chem.* **1976**, *5*, 207.
- Nagasawa, M.; Kagawa, I. *J. Polym. Sci.* **1957**, *25*, 61.
- Meiboom, S.; Gill, D. *Rev. Sci. Instrum.* **1958**, *29*, 688.
- Braun, S.; Kalinowski, H. O.; Berger, S. *150 and More Basic NMR Experiments: A Practical Course*; Wiley-VCH: Weinheim, 1998; p 159.
- Fabri, D.; Williams, M. A. K.; Halstead, T. K. *Carbohydr. Res.* **2005**, *340*, 889.
- Nagasawa, M.; Izumi, M.; Kagawa, I. *J. Polym. Sci.* **1958**, *37*, 375.
- Kern, W. *Makromol. Chem.* **1948**, *2*, 279.
- Anderson, C. F.; Record, M. T., Jr.; Hart, P. A. *Biophys. Chem.* **1980**, *7*, 301.
- Mulder, C. W.; Bleizer, J. D.; Leyte, J. C. T. *Chem. Phys. Lett.* **1980**, *69*, 354.
- Gustafsson, H.; Lindman, B.; Bull, T. *J. Am. Chem. Soc.* **1978**, *100*, 4655.
- Gustafsson, H.; Siegel, G.; Lindman, B.; Fransson, L. *FEBS Lett.* **1978**, *86*, 127.
- Minato, T.; Satoh, M. *J. Polym. Sci., Part B: Polym. Phys.* **2004**, *42*, 4412.
- Akitt, J. W. *NMR and Chemistry: An Introduction to Modern NMR Spectroscopy*, 3rd ed.; Chapman & Hall: London, 1992; p 87.
- Costa, D.; Ramos, M. L.; Burrows, H. D.; Tapia, M. J.; Miguel, M. *Chem. Phys.* **2008**, *352*, 241.
- Böhme, U.; Scheler, U. *Macromol. Symp.* **2004**, *211*, 87.
- Scheler, U. *Curr. Opin. Colloid Interface Sci.* **2009**, *14*, 212.
- Stilbs, P.; Furó, I. *Curr. Opin. Colloid Interface Sci.* **2006**, *11*, 3.
- Jeschke, G. *Curr. Opin. Solid State Mater. Sci.* **2003**, *7*, 181.
- Paul, A.; Griffiths, P. C.; Pettersson, E.; Stilbs, P.; Bales, B. L.; Zana, R.; Heenan, R. K. *J. Phys. Chem. B* **2005**, *109*, 15775.
- Böhme, U.; Scheler, U. *Macromol. Chem. Phys.* **2007**, *208*, 2254.
- Grass, K.; Böhme, U.; Scheler, U.; Cottet, H.; Holm, C. *Phys. Rev. Lett.* **2008**, *100*, 096104.
- Manning, G. S. *J. Chem. Phys.* **1969**, *51*, 924.
- Vidali, R.; Remoundaki, E.; Tsezos, M. *J. Colloid Interface Sci.* **2009**, *339*, 330.
- Li, X.; Englezos, P. *J. Colloid Interface Sci.* **2005**, *281*, 267.
- Companys, E.; Garcés, J. L.; Salvador, J.; Galceran, J.; Puy, J.; Mas, F. *Colloids Surf., A* **2007**, *306*, 2.
- Takashima, W.; Hayashi, K.; Kaneto, K. *Electrochem. Commun.* **2007**, *9*, 2056.
- Drosos, M.; Jerzykiewicz, M.; Deligiannakis, Y. *J. Colloid Interface Sci.* **2009**, *332*, 78.
- Pajarre, R.; Koukkari, P.; Räsänen, E. *J. Mol. Liq.* **2006**, *125*, 58.
- Koopal, L. K.; Saito, T.; Pinheiro, J. P.; van Riemsdijk, W. H. *Colloids Surf., A* **2005**, *265*, 40.
- Ge, Y.; MacDonald, D.; Sauvé, S.; Hendershot, W. *Environ. Model. Software* **2005**, *20*, 353.
- Scatchard, G. *Ann. N.Y. Acad. Sci.* **1949**, *51*, 660.
- Light, K. E. *Science* **1984**, *223*, 76.



- (63) Nicosia, S. *Pharmacol. Res. Commun.* **1988**, *20*, 733.
- (64) Zierler, K. *Trends Biochem. Sci.* **1989**, *14*, 314.
- (65) Crabbe, J. *Trends Biochem. Sci.* **1990**, *15*, 12.
- (66) Miyajima, T.; Ishida, K.; Katsuki, M.; Marinsky, J. A. *New Developments in Ion Exchange*; Kodansha-Elsevier: Tokyo, 1991. p 497.
- (67) Katchalsky, A.; Alexandrowicz, Z.; Kedem, O. *Chemical Physics of Ionic Solution*; Wiley: New York, 1966; p 295.
- (68) Huizenga, J. R.; Greiger, P. F.; Wall, F. T. *J. Am. Chem. Soc.* **1950**, *72*, 4228.
- (69) Strauss, U. P.; Ander, P. *J. Am. Chem. Soc.* **1958**, *80*, 6494.
- (70) Strauss, U. P.; Ross, P. D. *J. Am. Chem. Soc.* **1959**, *81*, 5299.
- (71) Chu, P.; Marinsky, J. A. *J. Phys. Chem.* **1967**, *71*, 4352.
- (72) Robinson, R. A.; Stokes, R. H. *Electrolyte Solutions*; Butterworths: London, 1959.
- (73) Kielland, J. *J. Am. Chem. Soc.* **1937**, *59*, 1675.
- (74) Rivas, B. L.; Pereira, E. D.; Moreno-Villoslada, I. *Prog. Polym. Sci.* **2003**, *28*, 173.
- (75) Burak, Y.; Ariel, G.; Andelman, D. *Curr. Opin. Colloid Interface Sci.* **2004**, *9*, 53.
- (76) Kijewska, I.; Hawlicka, E. *Carbohydr. Res.* **2005**, *340*, 1185.